



Thioredoxin reductase 3 suppression promotes colitis and carcinogenesis via activating pyroptosis and necrosis

Qi Liu¹ · Pengyue Du¹ · Yue Zhu¹ · Xintong Zhang¹ · Jingzeng Cai¹ · Ziwei Zhang^{1,2}

Received: 7 September 2021 / Revised: 1 January 2022 / Accepted: 17 January 2022 / Published online: 30 January 2022
© The Author(s), under exclusive licence to Springer Nature Switzerland AG 2022

Abstract

Background Txnrd3 as selenoprotein plays key roles in antioxidant process and sperm maturation. Inflammatory bowel diseases, such as ulcerative colitis and Crohn's disease, are becoming significantly increasing disease worldwide in recent years which are proved relative to diet, especially selenium intake.

Methods In the present study, 8-week-old C57BL/6N male Txnrd3^{-/-}, Txnrd3^{-/+}, Txnrd3^{+/+} mice, weight 25–30 g, were randomly chosen and each group with 30 mice. Feed 3.5% DSS drinking water and normal water continuously for 7 days. Mouse colon cancer cells (CT26) were cultured in vitro to establish Txnrd3 overexpressed/knocked-down model by cell transfection technology. Morphology and ultrastructure, calcium levels, ROS level, cell death were observed and detected in vivo and vitro.

Results In Txnrd3^{-/-} mice, ulcerative colitis was more severe, the morphological and ultrastructural lesions were also more prominent compared with wild-type mice, accompanied by the significantly increased expression of NLRP3, Caspase1, RIPK3, and MLKL. Overexpression of Txnrd3 could lead to increased oxidative stress through intracellular calcium outflow-induced oxidative stress increase followed by necrosis and pyroptosis pathway activation and further inhibit the growth and proliferation of colon cancer cells.

Conclusion Txnrd3 overexpression leads to intracellular calcium outflow and increased ROS, which eventually leads to necrosis and focal death of colon cancer cells, while causing Txnrd3^{-/-} mice depth of the crypt deeper, weakened intestinal secretion and immune function and aggravate the occurrence of ulcerative colitis. The present study lays a foundation for the prevention and treatment of ulcerative colitis and colon carcinoma in clinic treatment.

Keywords C57BL/6N · Ulcerative colitis · Colon cancer · Txnrd3 · Oxidative stress

Abbreviations

Selenium	Se
Txnrd3	Thioredoxin reductase 3
UC	Ulcerative colitis
IBD	Inflammatory bowel diseases
CRC	Colorectal cancer
DSS	Dextran sulfate sodium
siRNA	Small interfering RNA

DAI	Disease activity index
IOD	Integrated Optical Density

Background

Selenium (Se) as an essential micronutrient in both inorganic and organic forms is known to be incorporated into selenoproteins (25 in humans, 25 in gallus, 41 in fish and 24 in mice) in the form of selenocysteine (SEC) which plays important roles in antioxidant, reproduction, thyroid hormone formation and tumor prevention [1–3]. Among these selenoproteins, thioredoxin reductase family are known to participate in antioxidant process, regulation of intracellular redox potential and programmed cell death [4]. Three following members are included: Txnrd1, two mitochondrial thioredoxin reductase designated as Txnrd2 (TR3) and Txnrd3 (TR2, TrxR3 or TGR). TR1 is found located

✉ Ziwei Zhang
zhangziwei@neau.edu.cn

¹ College of Veterinary Medicine, Northeast Agricultural University, Harbin 150030, People's Republic of China

² Key Laboratory of the Provincial Education, Department of Heilongjiang for Common Animal Disease Prevention and Treatment, Northeast Agricultural University, Harbin 150030, People's Republic of China

within the cell content (cytosol/nucleus) [5]. Txnrd2 locates widespread but mostly in mitochondria. Previous studies in past years indicated that Txnrd3 specifically located in the testis [6, 7] and was proved to play important roles in reproduction, development of cancer and cardiovascular diseases [8–10]. However, interesting findings are proved for the first time in the present study that Txnrd3 could be expressed in mouse colon [11, 12]. As the incidence of intestinal diseases such as inflammatory bowel disease, ulcerative colitis and colorectal cancer is increasing year by year, great influence of dietary habits on human health is noticed [13]; role of selenium and selenoproteins especially Txnrd3 during inflammatory bowel disease and colon cancer is still unknown, which aroused our interests in further study.

Inflammatory bowel disease (IBD) has become a global public health concern occurs in young adults, in the form of Crohn's disease and ulcerative colitis (UC). Crohn's disease can affect the entire intestinal digestive tract from the mouth to anus; additionally, the development of inflammatory disease could also induce intestinal stenosis and fistula [14]. UC is known limited to colon with two important consequences: severe aggression and high risk of emergency surgery and bowel cancer, respectively. At present, the most reasonable concept of IBD pathogenesis is that gene susceptible individuals cannot tolerate environmental triggered intestinal flora disorders and chronic inflammation. Among the environmental factors associated with IBD, diet plays a key role in regulating the gut microbiota and influencing epigenetic changes, which can be used as a therapeutic tool to improve the course of disease [15]. Although excessive calories and some macronutrients proved promote intestinal inflammation, several micronutrients have the potential role to regulate intestinal inflammation [16]. As there are few dietary recommendations and weak evidence for disease prevention and management, immune nutrition has become a new concept as the raising importance of vitamins, β carotene and trace elements such as zinc, iron, manganese and selenium are involved in present study. Many studies over the years have linked selenium levels to the incidence and severity of intestinal diseases, such as IBD and colorectal cancer (CRC). CRC is the cancer type with second highest morbidity and mortality in Europe and worldwide. A large number of CRC risks may arise from dietary factors, genetic variations and their interactions [17, 18]. Unhealthy diet and lifestyles are the main causes of CRC [17, 19]. In David et al.'s research, observational and intervention results showed that selenium level relevance to the development risk of CRA and CRC, especially in selenium-deficient geographical areas like most parts of Europe [20–23]. Although relationship between IBD and environmental risk factors is still a subject needs in-depth study, diet and nutritional factors, especially Se, remain key factors to be valued.

As most selenoproteins have antioxidant properties, Se has long been thought to protect organs from inflammation and development of cancer by mitigating oxidative stress. Veronika et al. indicated that inadequate dietary intakes of Se could induce greater risk of cancer development in the colorectum. Txnrd family as selenoproteins are involved in several colon diseases. Recently, Song et al. found that increase of Txnrd1 effectively attenuates oxidative stress-induced injury of intestinal epithelial barrier [24]. However, another research indicated that there is no effect in TXNRDs activity during Se deprivation but GPX1 and SelP differentially decreased in contrast [25]. Clinical data also revealed that significant up-regulation of Txnrd1 was associated with poor prognosis in CRC patients [26]. Another survey claimed that Txnrd2 is a key gene interaction associated with colon cancer [27]. In Martha et al.'s research, Txnrd1 (3 SNPs) and Txnrd2 (3 SNPs) were proved to be associated with colon cancer; Txnrd2 (3 SNPs) and Txnrd3 (3 SNPs) were relative to rectal cancer; in addition, Txnrd1 and Txnrd3 were associated with colon cancer patients' survival in clinical terms [28]. However, the literature about Txnrd3 is scarce; its role, function and molecular mechanism during IBD and development of colon cancer are still unclear which aroused our great interest.

In the present study, animal model of ulcerative colitis in Txnrd3^{-/-}, Txnrd3^{-/+} and Txnrd3^{+/+} mice was constructed using DSS drinking water: over-expression and knockdown of Txnrd3 were constructed in vitro using CT26 colon cancer cell lines. Biological functions of Txnrd3 in intestinal tract are explored by various molecular biological and histomorphological methods by our studies. Present study aimed at exploring the role and mechanism of Txnrd3 during IBD and colon cancer development, which provides a favorable basis for colon cancer prevention and clinical treatment of patients with intestinal diseases.

Methods

No statistical methods were used to predetermine sample size. The experiments were not randomized and investigators were not blinded to allocation during experiments and outcome assessment.

Mice

Heterozygous Txnrd3[±] C57BL/6N mice were generated by a commercial supplier (Cyagen Biosciences, Santa Clara, CA, USA) using CRISPR/Cas-mediated genome engineering, which is used to design sgRNA, then high-throughput electro-transfer fertilized eggs to obtain Txnrd3[±] mice. Then adult female and male mice of non-nearest relatives with 25–30 g weight were chosen, and the female and male

knockout mice were placed in the same M1 size cage randomly at room temperature, 12 h illumination and 12 h darkness a day. The mice were fed with breeding materials and sterilized distilled water. All mouse experiments were approved by the institutional animal care and use committee and carried out in strict accordance with animal experiment standards defined by the laboratory animal center of Northeast Agricultural University. The Txnrd3 gene (NCBI Reference Sequence: NM-153162; Ensembl: ENSMUSG0000000811) located on Mouse chromosome 6. 16 exons were identified, with the ATG start codon in exon 1 and the TAG stop codon in exon 16 (Transcript: ENSMUST0000000828). Exon 2–5 was selected as target site. Cas9 and gRNA were co-injected into fertilized eggs for KO Mouse production. The pups were genotyped by PCR followed by sequencing analysis. Exon 2 starts from about 8.67% of the coding region. Exon 2–5 covers 18.92% of the coding region. The size of effective KO region is ~3896 bp. The KO region does not have any other known gene.

UC model

To construct a Dextran sulfate sodium (DSS)-induced colitis mouse model, 8-week-old male Txnrd3^{-/-}, Txnrd3^{+/-}, Txnrd3^{+/+} mice weighing between 25 and 30 g were randomly chosen and each group contained 30 mice. Mice were fed 5% DSS drinking water for 6 days, during this period mice intake foods and water freely, record daily weight, mental status, diet, hair color, stool characteristics, blood stool, diarrhea and weight loss. On the 6th day, mice developed obvious UC symptoms, all mice were sacrificed and colon tissue was collected and placed in the -80 °C refrigerator for further use. Disease assessment was calculated using disease activity index (DAI) as shown in Supplementary material Table 1.

Cell culture

CT26 cell line was purchased from in BNCC north biological cell library in the form of T25, culture bottle park in incubator for 4 h after received, abandon old medium, using PBS wash cells for twice, add 6-well plate 0.5 mL trypsin per well, check the status of cells under microscope till cells just fall off. The digestion was terminated with 12 mL CM2-1 culture medium (90% RPMI-1640 + 10% FBS) for passage, and the CT26 cells were gently blown, the plates were laid as following experiments required. For cryo storage, the digestion was terminated with 6 mL cryo solution (90% FBS + 10% DMSO), and the digestion was evenly blown. The tubes were divided into 6 cryo sterile storage tubes, which were cryo stored at -80 °C using program cooling box.

Cell transmission and transfection

After cells were plated 24 h, pcDNA3.1-plasmid, pcDNA3.1-Txnrd3 recombinant plasmid, siRNA-Txnrd3 mixed with lip2000 and RNAmix, then transfect into the cells. After 12 h of transfection, absorb the transfection reagent, wash cells with PBS for twice and add new CM2-1 medium. 24 h later collect the cells and finish follow-up qRT-PCR, Western blot, fluorescence staining etc. experiments. In addition, the pcDNA3.1-plasmid used in this article was purchased from Fenghui Bio (Changsha, China). Second, Txnrd3 with the flag label was synthesized by Biochemical and Biological Engineering (Shanghai, China), followed by PCR amplification, empty plasmid digestion, ligation, glue recovery and sequencing, and the recombinant pcDNA3.1-Txnrd3 plasmid was extracted with an endotoxin-free plasmid big-lift kit (TIANGEN, DP117, Beijing, China). siRNA-Txnrd3 was biosynthesized by RIBOBIO (Beijing, China). Finally pcDNA3.1-, pcDNA3.1-Txnrd3 and siRNA-Txnrd3 were transfected to CT26 cells with concentrations in pcDNA3.1-: Lipofectamine 2000 = 5 µL: 95 µL; pcDNA3.1-Txnrd3: Lipofectamine 2000 = 5 µL: 95 µL and siRNA: Lipofectamine RNAiMAX = 3 µL: 97 µL. Detailed sequences of pcDNA3.1-, pcDNA3.1-Txnrd3 and siRNA-Txnrd3 are shown in Supplementary Materials.

Detection the effect of Txnrd3 knockdown/overexpression on calcium ions in cells

The culture medium in the culture plate was discarded, incubated with Fluo-3AM and PBS for 45 min in 37 °C, loaded with fluorescent probe, then washed with PBS for once and then incubated in 37 °C incubator for 20 min to ensure the complete transformation of Fluo-3AM into cells. Finally, fluorescence microscope was used to observe and photograph. Image J was used to analyze the fluorescence intensity of each group.

Detection the effect of Txnrd3 knockdown/overexpression on reactive oxygen species assay in cells

DCFH-DA was diluted with serum-free 1640- RPMI at 1:1000. The final concentration is 10 µM mL⁻¹. Remove the old culture medium, add 1 mL diluted DCFH-DA. Then cells were incubated in a 37 °C cell incubator for 35 min. Cells were washed three times with serum-free medium to completely remove DCFH-DA that did not enter the cells. Fluorescence microscope using 488 nm as excitation wavelength and 525 nm as emission wavelength. Image J was used to analyze the fluorescence intensity of each group.

Detection the effect of Txnrd3 knockdown/ overexpression on apoptotic fluorescent Hoechst 33342/PI double staining

CT26 as adherent cells, present staining does not need to be digested with trypsin, discard the culture medium in the petri dish, wash with PBS for 2 times, add 5 μ L Hoechst staining solution and 5 μ L staining solution to each hole in turn, mix well, after 30 min of ice bath, using PBS to wash cells for once, then observe with fluorescence microscope red fluorescence and blue fluorescence. Image J was used to analyze the fluorescence intensity of each group.

Reagents and antibodies

Mouse antibodies used in present study are as follow: Anti-Caspase-1 antibody (Abcam, ab138483), Anti-NLRP3 antibody (Abcam, ab270449), Anti-MLKL Monoclonal Antibody (Proteintech, 66675-1-Ig), Anti-RIPK3 Polyclonal Antibody (Proteintech, 17563-1-AP), Anti-IL-1 β antibody (Abcam, ab234437). Hoechst 33342/PI was obtained from Invitrogen. Reactive oxygen species assay were purchased from Beyotime Biotechnology (S0033S). Fluo-3 AM was provided by Beyotime Biotechnology (S1056). Dextran sulfate sodium (DSS) was acquired from BBI Life Sciences Corporation (A600160-0050). All the reagents used in western blot were purchased from Solarbio Life Sciences. Cell culture reagents were purchased from Gibco.

Histopathological examination

After mice were killed on the 6th day, small-intestinal colon tissues from NC group and UC group 3 gene types mice were flushed with ice-cold PBS, rapidly fixed in 10% formaldehyde for 24 h and embedded in paraffin for microscopic examination later. 5- μ m-thick sections were cut from the prepared paraffin blocks, blocks were obtained, stained with hematoxylin and eosin (H&E) for further histopathological examination. Stained sections were observed and photographed using microscope.

TEM

The colon tissue from wild-NC, heterozygote-NC, homozygote-NC, wild-UC, heterozygote-UC, homozygote-UC ultrastructure was fixed with 2.5% glutaraldehyde phosphate buffer solution (v/v, pH 7.2) (1.0 \times 1.0 \times 1.0 mm) and 1% osmium tetroxide (v/v). The colon tissues from NC group 3 genotypes mice and UC group 3 genotypes mice were stained with 4.8% uranyl acetate. Then, the tissue was cut

into ultrathin sections, then installed, cleaned, impregnated, stained and incubated with lead citrate and analyzed by microscope. Transmission electron microscopy (GEM-1200 ES, Japan) was used to screen the micrographs.

Areal density of mouse intestinal during UC via IHC intensity

Colon tissues of three genotypes of mice (wild-type, heterozygous, and homozygous) in the normal and DSS drinking groups were used to determine the Areal density of IL-1 β , cleaved-Caspase3, Caspase1 was examined separately (positive cells stained brown). Data were analyzed using Image-pro plus 6.0 (Media Cybernetics, Inc., Rockville, MD, USA) software. Immunohistochemical optical density (AREAL DENSITY = IOD/AREA) was analyzed as follow, three 200 times visual field were randomly selected for each slice in each group. Fill the organization with the whole field of vision and ensure the background light of each photo is consistent. Using the Image-Pro Plus 6.0 software to select the same brown color as the unified standard to judge the positive percent in all photos, the cumulative optical density (IOD) and the pixel area (AREA) of each photo were obtained by analyzing percent of positive cells in each photo. The higher the AREAL DENSITY value is, the higher positive expression level in tissues will be.

Western blots

Western blot analysis was used to detect the expression of related proteins. Protein content in each sample of cells and tissues was determined by BCA method. Using RIPA lysate and PMSF in 100:1 ratio to prepare tissue homogenate and cell suspension. A pre-made 12% concentration of the SDS-PAGE gel, by SDS-polyacrylamide gel electrophoresis, transfer proteins into PVDF membrane in iced tranfection liquid for 2 h. Kept PVDF membrane at room temperature for 2 hours in defat milk. The antibodies were then diluted with BSA in the following proportions: Anti-Txnrd3(1:1000), Anti-Caspase-1(1:1000), Anti-NLRP3(1:1000), Anti-MLKL(1:1000), Anti-RIPK3(1:500), Anti-IL-1 β (1:1000), incubate antibodies and PVDF membrane stored at 4 $^{\circ}$ C for 12 h. Next, wash with TBST for four times, each time 15 min. A secondary antibody (1:10,000) IgG a rabbit bound to horseradish peroxidase, Santa Cruz, USA) 37 $^{\circ}$ C after incubation for 1 h, eluted with TBST four times, each time fifteen min. Finally, with the ECL kit (Kangweishiji Biotechnology, Beijing, China) to capture the final image. The β -actin content was analyzed as the loading control with a rabbit polyclonal antibody (1:1500, Santa Cruz Biotechnology, USA).

Quantitative PCR with reverse transcription

The template used in real-time quantitative PCR is reverse transcription products extracted from colon tissues and CT26 cells. The extraction process is shown in our previous experiment [29, 30], reverse transcription reaction was completed with a reverse transcription kit (Bioer Technology, Hangzhou, China). Expression of Txnrd3 was detected in colon tissue and transfected CT26 cells. The necrosis and pyroptosis pathway relative genes including NLRP3, ASC, Caspase1, GSDMD, IL-1 β , IL-18, RIPK1, RIPK3 and MLKL expression was detected. In addition, apoptosis pathway related genes including Caspase3, Caspase8, Bcl2 and Bax was also determined. The house keeping gene β -actin was used as reference in present study. Detailed primers information for the qRT-PCR assays is supplied in Supplementary Materials. Reaction mixtures were incubated in a LightCycler[®] 480 System (Roche, Basel, Switzerland). The PCR procedure was designed as follow: 1 cycle at 95 °C for 30 s and 35 cycles at 95 °C for 15 s and 60 °C for 30 s. The relative abundance of the mRNAs was analyzed using Pfaffl.

Determination of antioxidant enzyme activities and content in colon tissue

Free radical scavenging enzymes such as Total antioxidant capacity (T-AOC), Superoxide Dismutase (SOD), metabolizing enzymes such as Glutathione peroxidase (GSH-Px) and malondialdehyde (MDA) as an index of oxidative damage were determined to compare the differences between NC and UC colonies. Commercial assay kits for T-AOC, SOD, GSH-Px and MDA were provided by Jiancheng Biotechnology Research Institute (Nanjing, China). Measurements were performed according to the protocols provided by the manufacturer in the Laboratory of the Science and Technology Experiment Centre, Shanghai University of Traditional Chinese Medicine. The colon tissue was ground with electric homogenizer for subsequent detection. In addition, the CT26 cells were washed with PBS for twice; then the adherent cells on the culture plate were gently scraped with cell scraper, and the cell suspension was made using PBS for subsequent detection.

Statistical analysis

The data shown in the figures are mean \pm S.E.M.; except for the mouse weight curve, they are mean \pm S.D. All values are calculated from at least three independent biological replicates, unless specifically stated. For all tests (except survival curves), data were calculated using the survival curve performed under the log-rank test with 95% confidence intervals. Image J was used to analyze the fluorescence intensity

of each group. Statistical analysis was accomplished using Graphpad prism 8, SPSS19 and Microsoft Excel 2019.

Results

DSS—induced ulcerative colitis model established successfully

On 2nd day of 5%DSS treatment, mice began to appear unpleasant activity, body hair messy, loose stool and other symptoms. The disease activity index (DAI) value raised, with DAI mean of 3rd, 4th, 5th and 6th day in homozygous group were 2.4, 4.2, 8.0 and 10.6 respectively. On the 6th day, more than half of the animals lost more than 15% of their initial weight, all the mice developed diarrhea or showed fecal occult blood. The naked eye can see the perianal shapeless blood stool attachment of male mice in homozygous group. Compared with the wild-type mice in control group, heterozygous mice developed symptoms after 4 days of exposure to DSS aqueous solution; DAI score also showed a certain upward trend; however, the amplitude was not as significant as that of homozygous group, and all the results above were shown in Fig. 1A.

Effects of colitis model on intestinal tissue morphology in Txnrd3 knockout mice

As shown in Fig. 1B, in the normal drinking water group, three genotypes of mouse colonic mucosal epithelium were intact, the epithelial cells were normal and closely arranged, the lamina propria intestinal glands were abundant, and plenty of goblet cells were found. In addition, lymphocyte infiltration was seen in homozygous group (green arrow). DSS treatment induced ulcerative colitis group mice colon can be seen obvious abnormal structures, mucosal layer was observed ulcer (gray arrow), accompanied by a small number of lymphocytes and neutrophils infiltration (pink arrow) in wild group; heterozygous mice mucosal layer can be seen ulcer (green arrow), accompanied by a small number of lymphocytes and neutrophils infiltration (red arrow), some inflammatory cells infiltration into the submucosa, local intestinal gland dilatation (blue arrow); mice in homozygous group were observed further large area ulcers (green arrows) in the mucosal layer, intestinal glands disappeared and replaced by proliferative connective tissue (yellow arrows), and some goblet cells were destroyed (blue arrows). A small number of red blood cells (gray arrows) and epithelial cells (black arrows) were found in the intestinal cavity. In NC group, the intestinal crypt depth of wild-type, heterozygous and homozygous mice were 0.1042, 0.11044, and 0.1298, respectively. Wild-type, heterozygous, homozygous mice

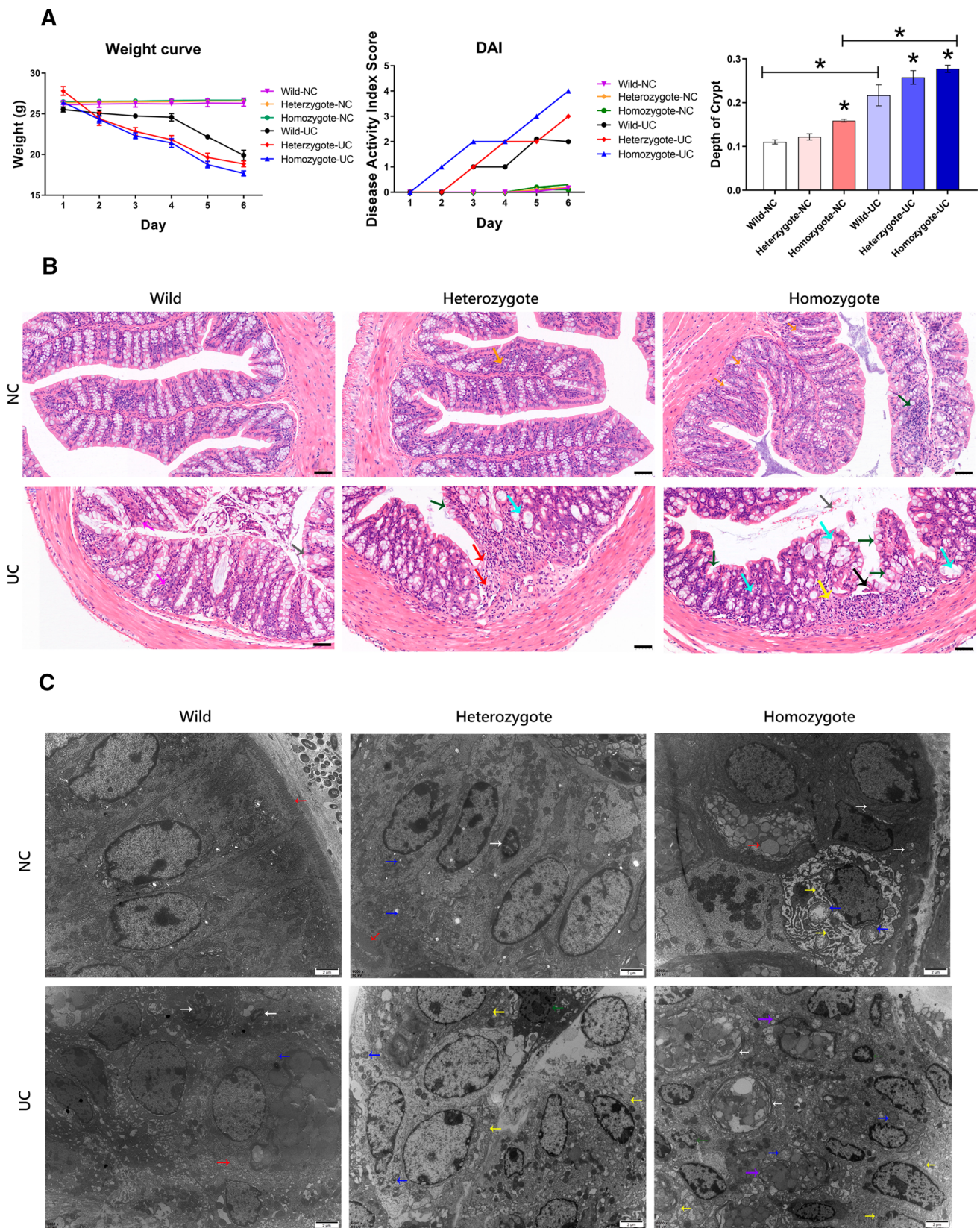


Fig. 1 Assessment of UC model in mice. **A** Daily weight loss and DAI score; **B** ultrastructure observation of colon in NC and UC group. Scale length is 50 μ m. Data represent mean \pm SEM. **C** Ultra-

structural observation of colon in 3 genotypes of NC and UC group. NC represents normal drinking water group, UC represents DSS drinking water group. Scale length is 2 μ m

in the UC group, the intestinal crypt depth was 0.21688, 0.0125786 and 0.2829, respectively.

Effects of colitis model on intestinal tissue ultrastructural structure in Txnrd3 knockout mice

In Fig. 1C, clear microvilli (red arrows) are observed in the colon of wild-type mice in the normal drinking water (NC) group by transmission electron microscopy. Cells structure was clear, neatly arranged and the number, size and morphology of organelles such as mitochondrial endoplasmic reticulum were normal. Heterozygous mouse colon cells were arranged neatly, with amount of microvilli reduced; number of mitochondria was regular, abnormal mitochondrial morphology (blue arrow) and occasional nuclear contraction (white arrow) were also observed. Homozygous mice colon tissue cells were randomly arranged and irregular, with abnormal mitochondrial morphology in slender strips, swelling and emptying of mitochondria, reduced fracture or disappearance of cristae (blue arrow), segregation in the pool of coarse endoplasmic reticulum (yellow arrow) and ER swelling (white arrow). DSS drinking water group wild-type mice colon tissue cell structure and boundaries are unclear, scattered, irregular, mitochondrial number increased deformation (blue arrow), individual cells approved deformation shrinkage (white arrow), endoplasmic reticulum swelling and pool isolation (red arrow); heterozygous colon tissue can be seen cell arrangement scattered nucleus deformation shrinkage, deep staining (green arrow), endoplasmic reticulum swelling (yellow arrow) and mitochondrial deformation (blue arrow). The colon structure of homozygous mice was irregular, the nucleus deformation wrinkle became smaller (green arrow), mitochondria swelling, ridge fracture or even disappearance (blue arrow), the number and volume of endoplasmic reticulum increased obviously, the morphology was swollen (yellow arrow), nucleus disappears and the organelles gradually dissolve into ruptured cells was seen (white arrow). In homozygote-UC group, purple arrows showed obvious rupture of cell membrane, cell contents flow out, swelling of mitochondria and endoplasmic reticulum which are regarded as iconic features of pyroptosis. In addition, transmission electron microscopy images showed subcellular features of necrotic-like swollen mitochondria.

Effects of colitis model on intestinal tissue immunohistochemical (IHC) in Txnrd3 knockout mice

In Fig. 2A and B, IHC results of wild-type, heterozygous, and homozygous mouse colitis of ulcerative colitis model

showed the expression level of IL-1 β in the homozygous group colon increased significantly during ulcerative colitis compared with that in the wild group ($p < 0.01$); the expression level of c-Capase3 also increased in the homozygous group and the difference was significant ($p < 0.05$); the expression level of Caspase1 also increased significantly in the homozygous group and the difference was extremely significant ($p < 0.01$). In addition, there was no significant difference between heterozygous group and control group.

Expression of Txnrd3 in colon tissues and transfected CT26 cells

Based on the results in Fig. 2C and D, Txnrd3 is stably expressed at both mRNA and protein levels in the colon of mice. Figure 2E shows that the Txnrd3 content in CT26 cells transfected with pcDNA3.1-Txnrd3 was 39.6 ± 1.2 -fold higher than that in pcDNA3.1-empty plasmid transfection group, and the Txnrd3 expression in CT26 after siRNA-Txnrd3 transfection was 0.15 ± 0.043 times compared with NC group. The above results indicate that Txnrd3 is stably expressed in colonic tissue and is successfully transfected in CT26 cells during Txnrd3 overexpression/knock-down.

Relationship between Txnrd3 and cell death in CT26 cells

As shown in Fig. 3, CT26 cells transfected with pcDNA3.1-Txnrd3 plasmids showed significant morphological changes and cell growth was inhibited or even died during the culture of CT26 cells. As Hoechst 33342 could penetrate the cell membrane, fluorescence of apoptotic cells after staining will be significantly enhanced than that in normal cells. Propidium iodide (PI) can not penetrate the cell membrane and can not be stained for normal cells with intact cell membranes. For necrotic cells, the integrity of their cell membranes was lost, and PI can stain necrotic cells. In Fig. 3, the proportion of positive cells PI staining increased significantly during Txnrd3 overexpression, while during Txnrd3 inhibition, positive cells in PI staining decreased significantly compare with control group. A small number of positive staining cells were also found in the control group, considering that the transfection reagent was also toxic to the cells.

Calcium concentration in CT26 cells during Txnrd3 knockout/overexpression Based on the same cell density in control, in Txnrd3 overexpression and Txnrd3 knock-down cells, the calcium content in the CT26 cells was significantly decreased in the Txnrd3 overexpression group than control group. As a result, Txnrd3 overexpression can cause intracellular calcium leakage while presented a slight increase of calcium in Txnrd3 knockout group as shown in Fig. 4A.

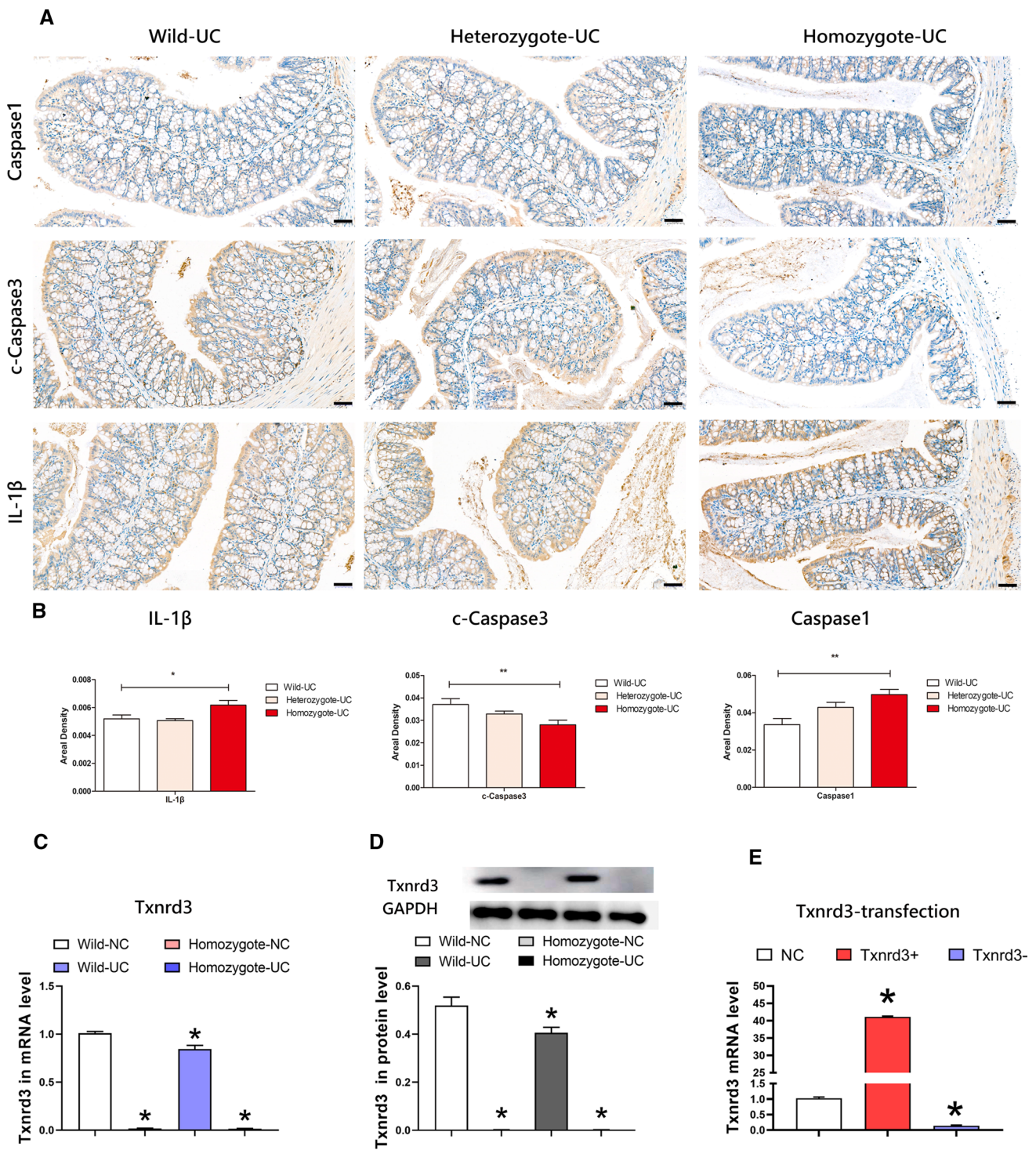


Fig. 2 IHC results of pyroptosis and inflammatory pathway factors. **A** Scale length is 50 μ m. **B** * representative difference is significant ($p < 0.05$), ** representative difference is extremely significant ($p < 0.01$). Data represent mean \pm SEM. **C** and **D** mRNA and protein expression of Txnr3 in colon tissue in Wild-NC, Homozygote-NC, Wild-UC and Homozygote-UC group. * representative difference

is extremely significant ($p < 0.01$). Data represent mean \pm SEM. **E** Expression of Txnr3 in NC, Txnr3+ and Txnr3- group during pcDNA3.1-, pcDNA3.1-Txnr3, siRNA-Txnr3 transfection. * representative difference is extremely significant ($p < 0.01$). Data represent mean \pm SEM

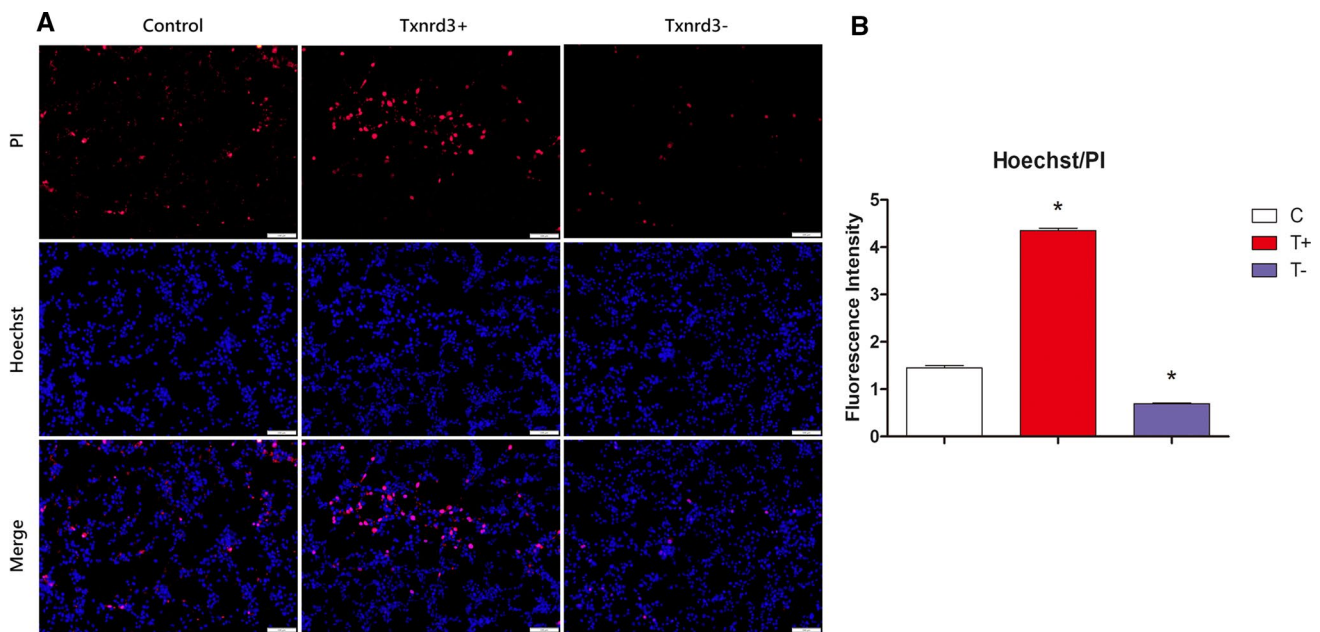


Fig. 3 Cell death in Txnrd3 transfected CT26 cells. Control represents CT26 cells transfected empty pcDNA3.1-plasmid, Txnrd3+ represent Txnrd3 overexpression group, Txnrd3- represent Txnrd3 knock-down group. Scale length is 100 μ m

Oxidative stress level in CT26 cells during Txnrd3 knockout/overexpression

In Fig. 4B, the results of ROS staining positive CT26 cells in the Txnrd3 overexpression group increased significantly compared with control group, while the proportion of green fluorescent cells in the Txnrd3 inhibition group increased slightly compared at the same time, but it was not significant as overexpressed. Considering Txnrd3 inhibition can also influence oxidative stress in CT26 cells.

Effects of Txnrd3 on mRNA expression of necrosis and pyroptosis pathway genes in colonies and CT26 cells

In the transfected CT26 cells, the expression levels of NLRP3, ASC, Caspase1, IL-1 β and IL-18 of pyrolytic-related genes in the Txnrd3 overexpression group were significantly higher than those in the control group with the difference especially significant ($p < 0.01$). The expression level of GSDMD increased significantly ($p < 0.05$); the expression of necrotizing pathway related gene MLKL, RIPK3 increased extremely significant ($p < 0.01$) in Txnrd3 overexpression group, however, the RIPK1 has no significant changes. The expression of apoptosis-related genes Bax, Caspase8 and Caspase3 was significantly increased ($p < 0.01$), and Bcl2 expression decreased significantly ($p < 0.05$). In the Txnrd3 inhibition group, expression of focal death gene NLRP3, ASC, IL-1 β decreased significantly, and the difference is extremely significant ($p < 0.01$);

GSDMD expression was significantly decreased ($p < 0.05$); RIPK3 expression significantly decreased ($p < 0.01$). In addition, expression of apoptosis-related gene Bax, Caspase8 increased significantly, while expression of Caspase3 and Bcl2 decreased at the same time ($p < 0.05$) (Fig. 5).

Detection of necrosis and pyroptosis pathway proteins in colonies and CT26 cells

As shown in Fig. 6A, B, in transfected CT26 cells the protein expression levels of GSDMD, RIPK3, MLKL, NLRP3, Caspase1 and IL-1 β in the Txnrd3 overexpression group were significantly higher than those in control group with the difference especial significant ($p < 0.01$). Expression of Caspase1 and MLKL was differentially decreased in Txnrd3 knockdown group ($p < 0.01$), but NLRP3 expression was increased at the same time ($p < 0.01$). Results indicated that Txnrd3 overexpression could lead to necrosis and pyroptosis in CT26 cells. In addition, homozygote-NC group relative protein expression in colons was differentially increased compared with wild-NC group ($p < 0.01$); expression of GSDMD, Caspase1, NLRP3, RIPK3, MLKL was up-regulated in wild-UC group ($p < 0.01$); GSDMD, Caspase1, NLRP3, RIPK3, MLKL was most differentially expressed in homozygote-UC group compared with wild-NC and wild-UC group ($p < 0.01$).

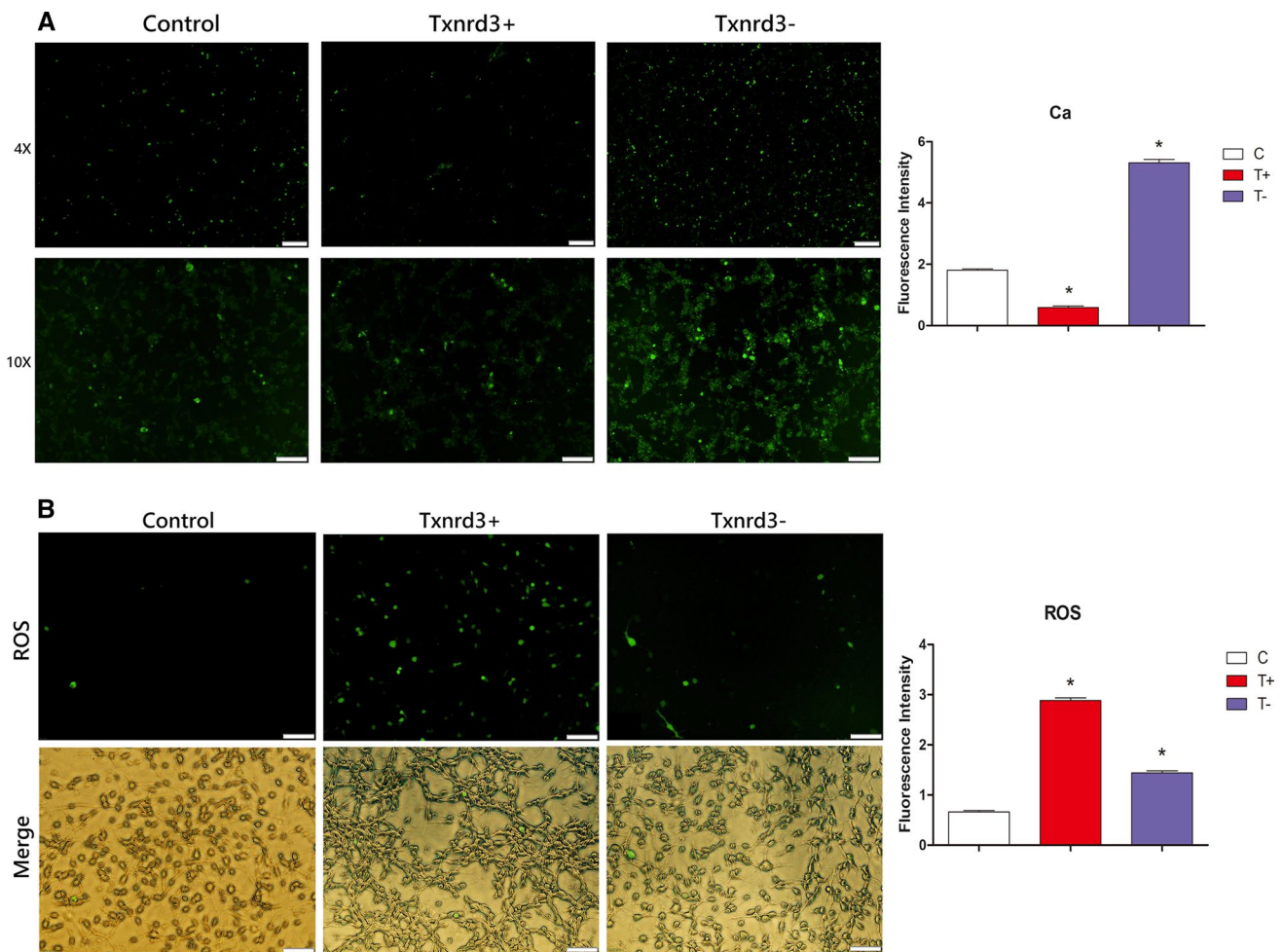


Fig. 4 Calcium and oxidative stress level in Txnrd3 transfected cells. **A** Calcium level in Txnrd3 transfected CT26 cells. Scale length is 200 μm . **B** Oxidative stress level in Txnrd3 transfected CT26 cells.

Control represents CT26 cells transfected empty pcDNA3.1-plasmid, Txnrd3+ represent Txnrd3 overexpression group, Txnrd3- represent Txnrd3 knock-down group. Scale length is 200 μm

Effects of Txnrd3 on oxidative stress in colon and Txnrd3 transfected CT26 cells

Which can be observed from Fig. 6C, D, antioxidant activity of transfected CT26 cells results showed that the SOD activity and T-AOC activity of Txnrd3 overexpression group differentially decreased 33.4% and 65.3% with significant difference ($p < 0.01$); with MDA content increased to 2.98 times ($p < 0.01$), the T-AOC activity in the Txnrd3 knockout group decreased 24.6%, MDA content increased 87.6%, SOD activity showed a downward state but the difference was not significant ($p > 0.05$). In vitro results of oxidative stress suggest that SOD activity and T-AOC activity of homozygote-NC group was differentially decreased 25.3% and 21.6% with significant difference compared with wild-NC group ($p < 0.01$), with MDA content increased to 1.4 times ($p < 0.01$). SOD activity and T-AOC activity of homozygote-UC group colon tissue decreased 41.6% and

47.9%, respectively, with MDA content increased to 1.97 times ($p < 0.01$).

Discussion

Selenium is playing important roles in antioxidant defense, formation of thyroid hormones, DNA synthesis, fertility and a chemoprevention agent for cancer. Selenoproteins as the active form of Se has close associations with colon cancer, which have attracted attention to role of selenoproteins in the process of several cancers [31, 32]. In vivo studies also demonstrated that dietary Se supplementation can reduce cancer incidence in animal models of melanoma and colon cancer. In recent study, 12 selenoproteins including GPX1, GPX4, Txnrd1, Txnrd2, Txnrd3 were found associated with CRC risk [33]. Kahlos et al. suggested that the up-regulation of thioredoxin and TrxR might contribute to drug resistance in

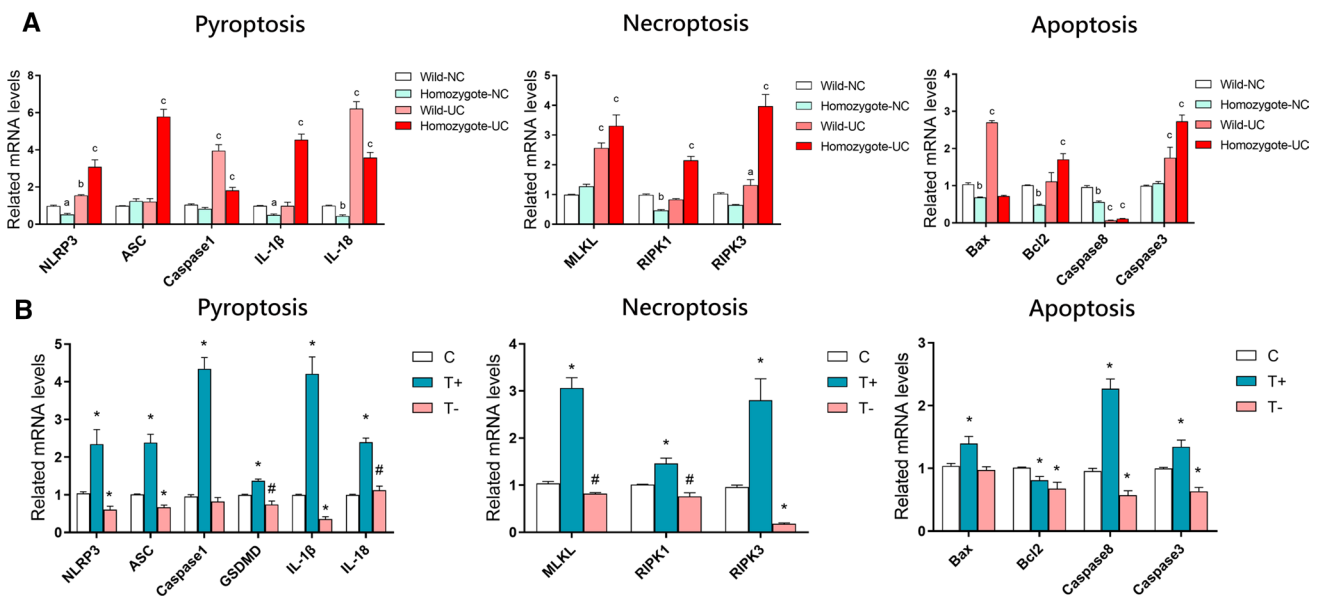


Fig. 5 Expression of pyroptosis, necroptosis and apoptosis pathway genes during Txnrd3 transfection in CT26 cells. C represents CT26 cells transfected empty pcDNA3.1-plasmid, T+ represent Txnrd3

overexpression group, T- represent Txnrd3 knock-down group. # representative difference is significant ($p < 0.05$), * representative difference is extremely significant ($p < 0.01$). Data represent mean \pm SEM

malignant cells [34]. Another research indicated that higher TrxR activity including Txnrd3 was found to enhance cellular antioxidant capacity and might also promote therapeutic resistance. Based on Liu et al.'s observations leukemia cells and liver cancer cells with overexpression of mtTxnrd3 were significantly less sensitive to erlotinib and gefitinib [35]. Due to the hierarchical pattern of organ-specific selenoproteins expressed under limited selenium supply conditions, tumor tissue-specific expression patterns may provide biomarkers of CRC risk, especially associated with insufficient selenium status. In Martha et al.'s research, Txnrd1, SeP15 and Txnrd3 were proved associated with survival after colon cancer diagnosis [12]. Other studies have routinely demonstrated significant reductions in serum Se levels in both child and adult UC and CD patients compared with healthy people [36–40]. In addition, another study showed that dietary selenium intake could depress the death rates of colon cancer [39, 41]. This possibility of selenium in prevent cancers requires further study in the future. However, the key task is how Txnrd3 could play a role in colon cancer?

Based on the present study results, we found that the depth of intestinal crypt of Txnrd3 $^{-/-}$ mice in homozygote-NC group was differentially increased compared with wild-NC group ($p < 0.05$), which was increased in heterozygote-NC group but with no differential difference ($p > 0.05$). In UC group, similar results were found. Then we come to the opinion that Txnrd3 knockdown could affect the formation of intestinal villi and the secretory function of epithelial cells, which eventually leads to the weakening of intestinal digestive function and immune barrier. As the depth of

intestinal crypt determines the ability of intestinal villi mitosis to produce epithelial cells, which reflects the rate of cell formation, as the cell maturity higher, the better secretory function will be. According to our results, depth of intestinal crypt decline indicating that during Txnrd3 knockdown the mucous membrane of mice may be damaged, intestinal digestion and absorption capacity decline, often accompanied by defecation or even blood stool. In addition, Txnrd3 knockdown induce elevated levels of ROS and decreased antioxidant capacity (SOD, MDA, T-AOC), subsequently increased oxidative stress in turn leads to colonic damage via activation of pyroptosis and necroptosis pathway genes. Above conclusions might be the reason of diarrhea, blood stool levels and other symptoms of Txnrd3 knockout mice in the DSS drinking water group significantly more severe than in the other groups.

Necroptosis and pyroptosis have been characterized as programmed cell death with necrotic morphologies such as rupture of plasma membrane. Pyroptosis, as a type of inflammatory programmed cell death, is mediated by multiple inflammasomes which can recognize danger signals and activate the secretion of pro-inflammatory cytokines like IL-18 and IL-1 β . It can induce cancer cell death within the gastrointestinal tract. Recent studies have indicated that inflammasomes could maintain intestinal homeostasis and defense the gastrointestinal (GI) tract from invasive pathogens. Otherwise its dysregulation might result in GI disorders such as inflammatory bowel disease and colon cancer. Clearly, inflammasomes like IL-18 and IL-1 β play emerging roles in the promotion of the integrity in

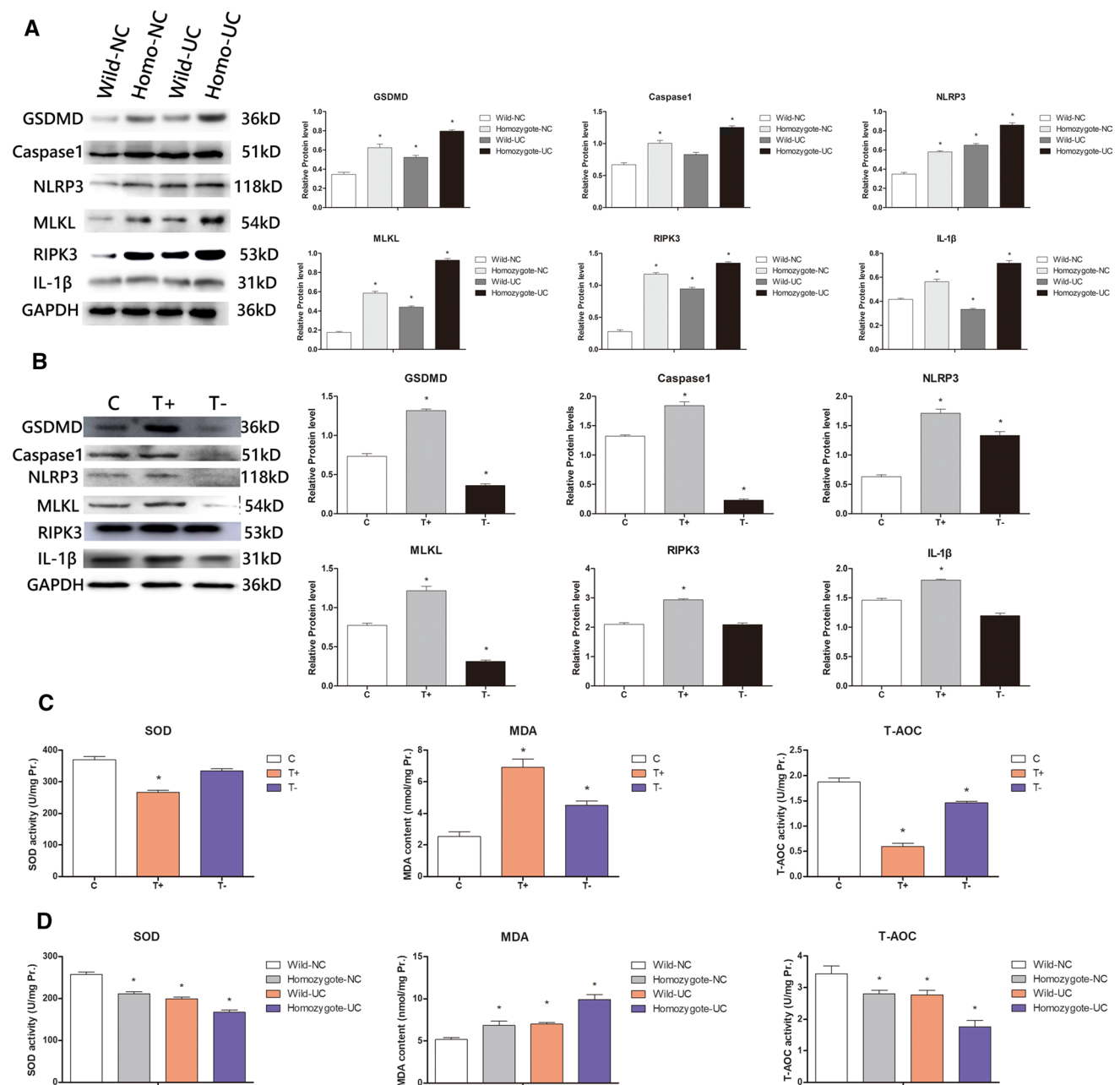


Fig. 6 Expression of cells death proteins, antioxidant capacity in colon and CT26 cells. **A, B** Expression of pyroptosis, necroptosis and apoptosis pathway proteins during Txnd3 transfection in CT26 cells. **C, D** Antioxidant capacity in Txnd3 transfected CT26 cells. **C** represents

CT26 cells transfected empty pcDNA3.1-plasmid, T+ represents Txnd3 overexpression group, T- represents Txnd3 knock-down group. * Representative difference is significant ($p < 0.05$). Data represent mean \pm SEM

intestinal epithelium and immune barrier via pyroptosis pathway in tumor cells. In the present study, we observed that Txnd3 overexpression in CT26 mouse colon cancer cells showed outflow of calcium with the endoplasmic reticulum stress, further induce elevated levels of ROS and decreased antioxidant capacity (SOD, MDA, T-AOC), subsequently increased oxidative stress in turn leads to necroptosis and pyroptosis pathway genes activation. In

addition, knockdown Txnd3 in CT26 cells showed opposite results, the colon cancer cell survival rate raise up, the growth is rapid and further exacerbates the colon cancer development. These findings are consistent with the results of in vivo experiments, which preliminarily verifies our hypothesis that knockout of Txnd3 could aggravate ulcerative colitis and promote the growth of colon cancer cells. Supplemental Txnd3 via transfection technology in

cells could inhibit the growth of colon cancer cells in vitro and induce necrosis and pyroptosis of CT26 cells. It provides a theoretical basis for reducing inflammatory bowel disease and preventing colon cancer.

Although our group established Txnrd3 knockout mice for the first time in this experiment and explored the function and mechanism of Txnrd3 in inflammatory bowel disease and colon cancer, we know that there are still some limitations. Subsequent experiments should be further carried out, such as miRNAome analyze, as recent data have implicated miRNAs in immune response to bacteria invasion and the differential regulation of cytokines. Researches indicated that miRNA dysregulation play a role in IBD, in addition, miRNAs have also been shown to regulate intestinal barrier integrity during UC development. In addition, the knockout of Txnrd3 can aggravate the development of inflammatory bowel disease in vivo and overexpression of Txnrd3 should lead to cell necrosis in CT26 mouse colon cancer cells in vitro, and whether dietary selenium supplementation can alleviate the development of inflammatory bowel disease and role of Txnrd3 in non-cancerous colon cells remains to be further verified.

Conclusions

We show for the first time that a stable reproduction Txnrd3 knockout mouse model is successfully established. In addition, we also proved that Txnrd3 is not specifically expressed in the testis in the traditional sense, but also in the colon. The overexpression of Txnrd3 in vitro can induce pyroptosis and necrosis of CT26 cells by regulating the imbalance of calcium homeostasis and oxidative stress. In summary, Txnrd3 can be used as a clinical diagnostic index of inflammatory bowel disease and provide theoretical basis for the practice of nutritional immunotherapy.

Supplementary Information The online version contains supplementary material available at <https://doi.org/10.1007/s00018-022-04155-y>.

Acknowledgements The contents of this manuscript are solely the responsibility of the authors and do not necessarily represent the official view of the Northeast Agricultural University. We would like to acknowledge the contributions and support of Pro. Shiwen Xu, Pro. Hongjin Lin and Dr. Mengrao Guo in present study.

Author contributions Conceived and designed the experiments: Ziwei Zhang, Qi Liu. Performed the experiments: Qi Liu, Yue Zhu, Xintong Zhang. Analyzed the data: Pengyue Du, Jingzeng Cai. Contributed reagents /materials/analysis tools: Ziwei Zhang. Wrote the paper: Qi Liu.

Funding This work was supported by the National Natural Science Foundation of China [grant number 31872531].

Availability of data and materials All the data underlying this article are available in the article and in its online supplementary material.

Code availability Manuscript was written using Microsoft Word 2010; Figures were achieved via Photoshop CS5. Data analysis and graph drawing were finished with Graphpad Prism 8.

Declarations

Conflict of interest The authors declare no competing financial interests.

Ethics approval and consent to participate Animal care and experimental procedures were performed with approval from the Northeast Agricultural University Institutional Animal Care and Use Committee.

Consent for publication Not applicable.

References

1. Wang W, Shi Q, Wang S, Zhang H, Xu S (2020) Ammonia regulates chicken tracheal cell necroptosis via the LncRNA-107053293/MiR-148a-3p/FAF1 axis. *J Hazard Mater* 386:121626
2. Chi Q, Zhang Q, Lu Y, Zhang Y, Xu S, Li S (2021) Roles of selenoprotein S in reactive oxygen species-dependent neutrophil extracellular trap formation induced by selenium-deficient arteritis. *Redox Biol* 44:102003
3. Kryukov GV, Castellano S, Fau-Novoselov SV, Novoselov SV, Fau-Lobanov AV, Lobanov AV, Fau-Zehtab O, Zehtab O, Fau-Guigó R, Guigó R, Fau-Gladyshev VN et al (2003) Characterization of mammalian selenoproteomes. *Science* 300(5624):1439–1443
4. Fomenko DE, Xing W, Adair BM, Thomas DJ et al (2007) High-throughput identification of catalytic redox-active cysteine residues. *Science* 315(5810):387–389
5. Li J, Zhang W, Zhou P, Tong X, Guo D, Lin H (2021) Selenium deficiency induced apoptosis via mitochondrial pathway caused by Oxidative Stress in porcine gastric tissues. *Res Vet Sci* 1:S0034-5288(21)00305-2
6. Sun QA, Wu Y, Zappacosta F, Jeang KT, Lee BJ, Hatfield DL et al (1999) Redox regulation of cell signaling by selenocysteine in mammalian thioredoxin reductases. *J Biol Chem* 274(35):24522
7. Fairweather-Tait SJ, Collings R, Hurst R (2010) Selenium bioavailability: current knowledge and future research requirements. *Am J Clin Nutr* 91(5):1484S-1491S
8. Davis CD, Tsuji PA et al (2012) Selenoproteins and cancer prevention. *Ann Rev Nutr* 32:73–95
9. Fairweather-Tait SJ, Bao Y, Broadley MR, Collings R, Hurst R (2011) Selenium in human health and disease. *Antioxid Redox Signal* 14(7):1337–1383
10. Rayman MP (2012) Selenium and human health. *Lancet* 379(9822):1256–1268
11. Slattery ML, Lundgreen A, Welbourn B, Corcoran C, Wolff RK (2012) Genetic variation in selenoprotein genes, lifestyle, and risk of colon and rectal cancer. *PLoS ONE* 7(5):e37312
12. Hughes D, Kunická T, Schomburg L, Liška V, Swan N, Souček P (2018) Expression of selenoprotein genes and association with selenium status in colorectal adenoma and colorectal cancer. *Nutrients* 10(11):1812

13. Short SP, Pilat JM, Williams CS (2018) Roles for selenium and selenoprotein P in the development, progression, and prevention of intestinal disease. *Free Radical Biol Med* 127:26–35
14. Aleksandrova K, Romero-Mosquera B, Hernandez V (2017) Diet, gut microbiome and epigenetics: emerging links with inflammatory bowel diseases and prospects for management and prevention. *Nutrients* 9(9):962
15. Kostic AD, Xavier RJ, Gevers D (2014) The microbiome in inflammatory bowel disease: current status and the future ahead. *Gastroenterology* 146(6):1489–1499
16. Lee D, Albenberg L, Compher C, Baldassano R, Piccoli D, Lewis JD et al (2015) Diet in the pathogenesis and treatment of inflammatory bowel diseases. *Other* 148(6):1087–1106
17. Vita MD (2013) Strong correlation between diet and development of colorectal cancer. *Front Biosci* 18(1):190–198
18. Slattery ML, Lundgreen A, Herrick JS, Caan BJ, Potter JD, Wolff RK (2011) Diet and colorectal cancer: analysis of a candidate pathway using SNPs, haplotypes, and multi-gene assessment. *Nutr Cancer* 63(8):1226–1234
19. Ferlay J, Soerjomataram I, Fau-Dikshit R, Dikshit R, Fau-Eser S, Eser S, Fau-Mathers C, Mathers C, Fau-Rebello M, Rebello M, Fau-Parkin DM et al (2015) Cancer incidence and mortality worldwide: sources, methods and major patterns in GLOBOCAN 2012. *Int J Cancer* 136(5):E359–E386
20. Fedirko V, Jenab M, Méplan C, Jones JS, Zhu W, Schomburg L et al (2019) Association of selenoprotein and selenium pathway genotypes with risk of colorectal cancer and interaction with selenium status. *Nutrients* 11(4):935
21. Méplan C, Hesketh J (2014) Selenium and cancer: a story that should not be forgotten—insights from genomics. *Cancer Treat Res* 159(159):145–166
22. Hughes DJ, Fedirko V, Jenab M, Schomburg L, Hesketh JE (2014) Selenium status is associated with colorectal cancer risk in the European prospective investigation of cancer and nutrition cohort. *Int J Cancer* 136(5):1149–1161
23. Gerald FC (2015) Biomarkers of selenium status. *Nutrients* 7(4):2209–2236
24. Song D, Lu Z, Wang F, Wang Y (2017) Biogenic nano-selenium particles effectively attenuate oxidative stress-induced intestinal epithelial barrier injury by activating the Nrf2 antioxidant pathway. *J Anim Sci* 9(17):14724–14740
25. Joan CS, David MA, Teresa BM, Mickael B, Eric P, Ruth F et al (2019) 2-Hydroxy-(4-methylseleno)butanoic acid is used by intestinal Caco-2 cells as a source of selenium and protects against oxidative stress. *J Nutr* 149:2191–2198
26. Clab E, Yze B, Jw C, Yy D, Yz J, Xq I et al (2020) FoxO3 reverses 5-fluorouracil resistance in human colorectal cancer cells by inhibiting the Nrf2/TR1 signaling pathway. *Cancer Lett* 470:29–42
27. Slattery ML, Pellatt DF, Wolff RK, Lundgreen A (2016) Genes, environment and gene expression in colon tissue: a pathway approach to determining functionality. *Int J Mol Epidemiol Genet* 7(1):45–57
28. Slattery ML, Abbie L, Bill W, Christopher C, Wolff RK, Hold GL (2012) Genetic variation in selenoprotein genes, lifestyle, and risk of colon and rectal cancer. *PLoS ONE* 7(5):e37312
29. Liu Q, Yang J, Gong Y, Cai J, Zhang Z (2019) Role of miR-731 and miR-2188–3p in mediating chlorpyrifos induced head kidney injury in common carp via targeting TLR and apoptosis pathways. *Aquat Toxicol* 215:105286
30. Liu Q, Yang J, Gong Y, Cai J, Zheng Y, Zhang Y et al (2020) MicroRNA profiling identifies biomarkers in head kidneys of common carp exposed to cadmium. *Chemosphere* 247:125901
31. Greenwald P, Milner JA, Anderson DE, McDonald SS (2002) Micronutrients in cancer chemoprevention. *Cancer Metastasis Rev* 21(3–4):217–230
32. Stratton MS, Reid ME, Schwartzberg G, Minter FE, Monroe BK, Alberts DS et al (2003) Selenium and inhibition of disease progression in men diagnosed with prostate carcinoma: study design and baseline characteristics of the “Watchful Waiting” Study. *Anticancer Drugs* 14(8):595–600
33. Catherine M (2015) Selenium and chronic diseases: a nutritional genomics perspective. *Nutrients* 7(5):3621–3651
34. Kahlos K, Soini Y, Fau-Säily M, Säily M, Fau-Koistinen P, Koistinen P, Fau-Kakko S, Kakko S, Fau-Pääkkö P, Pääkkö P, Fau-Holmgren A et al (2001) Up-regulation of thioredoxin and thioredoxin reductase in human malignant pleural mesothelioma. *Int J Cancer* 95(3):198–204
35. Chen X, Bi M, Yang J, Cai J, Zhang H, Zhu Y et al (2021) Cadmium exposure triggers oxidative stress, necroptosis, Th1/Th2 imbalance and promotes inflammation through the TNF- α /NF- κ B pathway in swine small intestine. *J Hazard Mater* 20;421:126704
36. Liu XJ, Wang YQ, Shang SQ, Xu SW, Guo MY (2022) TMT induces apoptosis and necroptosis in mouse kidneys through oxidative stress-induced activation of the NLRP3 inflammasome. *Ecotoxicol Environ Saf* 230:113167
37. Geerling BJ, Badart-Smook A, Stockbrügger RW, Brummer RJM (2000) Comprehensive nutritional status in recently diagnosed patients with inflammatory bowel disease compared with population controls. *Eur J Clin Nutr* 54(6):514–521
38. Ojuawo A, Keith L (2002) The serum concentrations of zinc, copper and selenium in children with inflammatory bowel disease. *Cent Afr J Med* 48(9–10):116–119
39. Kuroki F, Matsumoto T, Iida M (2003) Selenium is depleted in Crohn’s disease on enteral nutrition. *Dig Dis* 21(3):266–270
40. Teresa AT, Miguel N-A, Javier QG, Cristina SS, José R-H, Flor NL (2016) Ulcerative colitis and Crohn’s disease are associated with decreased serum selenium concentrations and increased cardiovascular risk. *Nutrients* 8(12):780
41. Lener MR, Gupta S, Scott RJ, Tootsi M, Ski JL (2013) Can selenium levels act as a marker of colorectal cancer risk? *BMC Cancer* 13(1):214

Publisher's Note Springer Nature remains neutral with regard to jurisdictional claims in published maps and institutional affiliations.